The Astrophysical Journal, 671:1708–1716, 2007 December 20


# HYPERVELOCITY STARS. III. THE SPACE DENSITY AND EJECTION HISTORY OF MAIN-SEQUENCE STARS FROM THE GALACTIC CENTER

Warren R. Brown, Margaret J. Geller, Scott J. Kenyon, and Michael J. Kurtz
Smithsonian Astrophysical Observatory, 60 Garden Street, Cambridge, MA 02138; wbrown@cfa.harvard.edu, mgeller@cfa.harvard.edu, skenyon@cfa.harvard.edu, mkurtz@cfa.harvard.edu

and

Benjamin C. Bromley
Department of Physics, University of Utah, 115 S 1400 E, Room 201, Salt Lake City, UT 84112; bromley@physics.utah.edu
*Received 2007 August 10; accepted 2007 September 7*

## ABSTRACT

We report the discovery of three new unbound hypervelocity stars (HVSs), stars traveling with such extreme velocities that dynamical ejection from a massive black hole (MBH) is their only suggested origin. We also detect a population of possibly bound HVSs. The significant asymmetry we observe in the velocity distribution—we find 26 stars with $v_{\rm rf} > 275$ km s$^{-1}$ and one star with $v_{\rm rf} < -275$ km s$^{-1}$—shows that HVSs must be short-lived, probably 3–4 $M_\odot$ main-sequence stars. Any population of hypervelocity post-main-sequence stars should contain stars falling back onto the Galaxy, contrary to the observations. The spatial distribution of HVSs also supports the main-sequence interpretation: longer lived 3 $M_\odot$ HVSs fill our survey volume; shorter lived 4 $M_\odot$ HVSs are missing at faint magnitudes. We infer that there are $96 \pm 10$ HVSs of mass 3–4 $M_\odot$ within $R < 100$ kpc, possibly enough HVSs to constrain ejection mechanisms and potential models. Depending on the mass function of HVSs, we predict that SEGUE may find up to 5–15 new HVSs. The travel times of our HVSs favor a continuous ejection process, although a ~120 Myr old burst of HVSs is also allowed.

*Subject headings:* Galaxy: center — Galaxy: halo — Galaxy: kinematics and dynamics — Galaxy: stellar content — stars: early-type

*Online material:* machine-readable table

## 1. INTRODUCTION

In 2005 we discovered the first HVS: a 3 $M_\odot$ main-sequence star traveling with a Galactic rest-frame velocity of at least $+709 \pm 12$ km s$^{-1}$, many times the escape velocity of the Galaxy at its heliocentric distance of 110 kpc (Brown et al. 2005; Fuentes et al. 2006). This star cannot be explained by normal stellar interactions: the maximum ejection velocity from binary disruption mechanisms (Blaauw 1961; Poveda et al. 1967) is limited to ~300 km s$^{-1}$ for few $M_\odot$ stars (Leonard 1991, 1993; Tauris & Takens 1998; Portegies Zwart 2000; Davies et al. 2002; Gualandris et al. 2005). Thus the origin of the HVS must be tied to a more massive and compact object.

Hills (1988) first predicted HVSs as an inevitable consequence of three-body interactions with a massive black hole (MBH). There is overwhelming evidence for a $4 \times 10^6$ $M_\odot$ MBH at the center of our Galaxy (Schödel et al. 2003; Ghez et al. 2005). Thus HVSs are probably stars ejected from the Galaxy by the MBH in the Galactic center.

Further HVS discoveries have followed the original discovery. Hirsch et al. (2005) reported a helium-rich subluminous O star leaving the Galaxy with a rest-frame velocity of at least +717 km s$^{-1}$. Edelmann et al. (2005) reported an 8 $M_\odot$ main-sequence star with a Galactic rest-frame velocity of at least +548 km s$^{-1}$, possibly ejected from the Large Magellanic Cloud. Brown et al. (2006a, 2006b [hereafter Paper I], 2007b [hereafter Paper II]) designed a targeted HVS survey using the 6.5 m MMT and Whipple 1.5 m telescopes to measure the radial velocities of distant B-type stars. This strategy has worked remarkably well, yielding seven HVSs and evidence for a bound population of stars ejected by the same mechanism. Here we report the three newest HVS discoveries, and discuss additional evidence for the "bound" HVSs.

The existence of HVSs has inspired broad theoretical interest, and many testable predictions have emerged. It is clear that HVSs can be ejected by different mechanisms: binary star encounters with a single MBH (Hills 1988; Yu & Tremaine 2003; Bromley et al. 2006) or possibly with an intermediate-mass black hole (IMBH; Gualandris & Portegies Zwart 2007); single star encounters with a binary MBH (Yu & Tremaine 2003; Sesana et al. 2006, 2007a; Merritt 2006) or an inspiraling IMBH-MBH (Gualandris et al. 2005; Levin 2006; Baumgardt et al. 2006); and single star encounters with the cluster of stellar mass black holes around the MBH (O'Leary & Loeb 2008). The dominant ejection mechanism remains unclear. Ejection rates depend on the number of stars scattered onto orbits that intersect the MBH's "loss cone" (Perets et al. 2007; Perets & Alexander 2007). Interestingly, the different ejection mechanisms result in different distributions of HVS ejection velocities and ejection rates (e.g., Yu & Tremaine 2003; Sesana et al. 2007b).

HVSs probe a variety of characteristics of the Galaxy. The density of HVSs and their distribution of velocities tell us about the MBH's environment. The stellar types of HVSs tell us about the types of stars orbiting near the MBH (Brown et al. 2006a; Demarque & Virani 2007; Kollmeier & Gould 2007; Lu et al. 2007). The trajectories of HVSs provide unique probes of the shape and orientation of the Galaxy's dark matter halo (Gnedin et al. 2005; Yu & Madau 2007). A large sample of HVSs will be a new and powerful tool to investigate these issues.

Our HVS radial velocity survey is now 96.5% complete for faint B-type stars over 7300 deg$^2$ of the Sloan Digital Sky Survey (SDSS) Data Release 5 (DR5; Adelman-McCarthy et al. 2007).

Our survey provides strong evidence for a class of HVSs on bound orbits (Paper II) matching expectations from theoretical models (Bromley et al. 2006; Sesana et al. 2007b). The distribution of HVSs on the sky appears marginally anisotropic, as expected for a magnitude-limited survey of HVSs ejected from the Galactic center (Paper II).

Here we address the HVS's stellar type, their space density, and the history of HVS ejections from the Galactic center. In § 2 we discuss the final target selection and spectroscopic identifications. In § 3 we describe three new HVSs. In § 4 we show that the observed HVSs must be short-lived objects, probably main-sequence stars. In § 5 we calculate the space density of HVSs, and predict HVS discovery rates for some future surveys. In § 6 we calculate HVS travel times, and discuss their ejection history. We conclude in § 7. The new observations are in the Appendix.

## 2. DATA

### 2.1. *Target Selection*

Paper I describes the target selection for our survey of faint $17 < g_0' < 19.5$ HVS candidates. Briefly, we use SDSS photometry to select HVS candidates with the colors of late B-type stars. B-type stars have lifetimes consistent with travel times from the Galactic center but are not a normally expected Galactic halo population. Our color selection introduces no kinematic bias and allows for stars at any velocity.

In this paper we make two changes to the Paper I target selection: (1) we select targets from the larger SDSS DR5 catalog, and (2) we include stars in a supplementary color-color region defined by $0.55 < (u' - g')_0 < 0.9$ and $-0.28 < (g' - r')_0 < -0.25$ (see Fig. 1). Our full target list contains 621 HVS candidates over 7300 deg$^2$ of sky. We have observed 575 of these targets; we are thus 93% complete for the faint HVS candidates. The remaining 46 targets are confined to the region $13.25^{\rm h} <$ R.A. $< 14.5^{\rm h}$.

Paper II describes the target selection for our complementary survey of bright $15 < g_0' < 17$ HVS candidates. We now select targets from the SDSS DR5 catalog. We identify a total of 892 objects with B-type colors; 691 satisfy our Galactic longitude and latitude cut. We have observed all 691 objects and are thus 100% complete for bright HVS candidates. These objects are spread over the identical 7300 deg$^2$ of sky as the faint HVS candidates.

### 2.2. *Spectroscopic Observations*

New observations of faint HVS candidates were obtained at the 6.5 m MMT telescope with the MMT Blue Channel spectrograph on the nights of 2006 December 21–26, 2007 March 18–20, and 2007 May 14–18. We operated the spectrograph with the 832 line mm$^{-1}$ grating in second order and a 1.25″ slit. These settings provide wavelength coverage 3650–4500 Å and a spectral resolution of 1.2 Å. Exposure times ranged from 5 to 30 minutes and yielded a signal-to-noise ratio (S/N) = 15 in the continuum at 4000 Å. We obtained comparison lamp exposures after every exposure.

We also obtained new observations of bright HVS candidates at the Whipple Observatory 1.5 m Tillinghast telescope with the FAST spectrograph (Fabricant et al. 1998) over the course of 11 nights spread between 2006 September and 2007 May. We operated the spectrograph with a 600 line mm$^{-1}$ grating and a 2″ slit. These settings provide wavelength coverage 3500–5400 Å and a spectral resolution of 2.3 Å. Like the MMT observations, exposure times ranged from 5 to 30 minutes and yield S/N = 15 in the continuum at 4000 Å. We obtained comparison lamp exposures after every exposure.

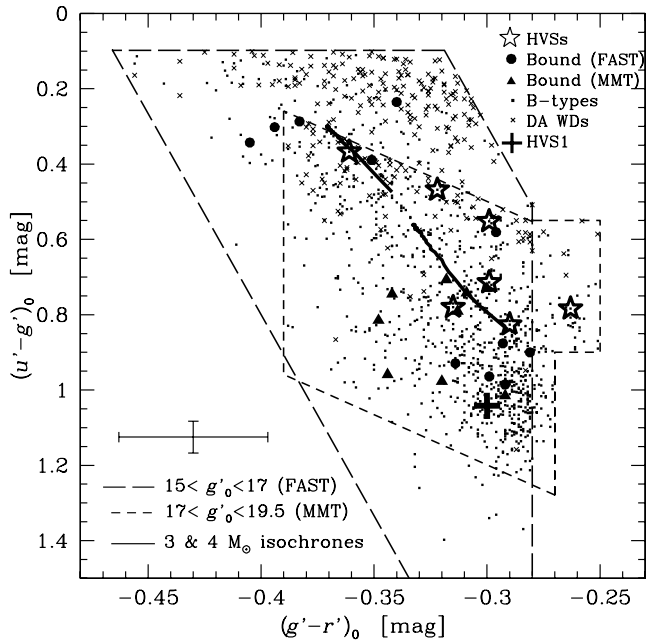


FIG. 1.—Color-color diagram showing the spectroscopic identifications of the 1005 late-B spectral type stars (*squares*) and the 244 white dwarfs (*crosses*) in our survey. Target selection regions are shown for the MMT (*short-dashed line*) and FAST (*long-dashed line*) samples. If the HVSs (*stars*) are main-sequence stars, then Girardi et al. (2004) stellar evolution tracks suggest they are 3 $M_\odot$ (*lower solid line*) or 4 $M_\odot$ stars (*upper solid line*). The average color uncertainties are illustrated by the error bar on the lower left. Also marked are the 19 possibly bound HVSs in the MMT sample (*triangles*) and FAST sample (*circles*), and HVS1 ( *plus sign*).

We extracted the spectra using IRAF[1] in the standard way and measured radial velocities using the cross-correlation package RVSAO (Kurtz & Mink 1998). Brown et al. (2003) describe the cross-correlation templates we use. The radial velocity accuracy is ±11 km s$^{-1}$ for the B-type stars.

### 2.3. *Spectroscopic Identifications*

Figure 1 plots the colors and spectroscopic identifications of the 1266 HVS candidates in our survey. We find that 1005 (79.4%) are stars of B spectral type and 244 (19.3%) are DA white dwarfs. Curiously, the white dwarfs in our survey have very unusual colors for DA white dwarfs; these colors imply very low surface gravity. Indeed, a detailed analysis of the spectra reveals that one of the white dwarfs has a mass of 0.17 $M_\odot$, the lowest mass white dwarf ever found (Kilic et al. 2007a, 2007b). Other remarkable objects include B supergiants in the Leo A dwarf galaxy (Brown et al. 2007a) and one compact, extremely metal-poor galaxy with properties similar to the host galaxies of nearby gamma-ray bursts (Kewley et al. 2007; Brown et al. 2008).

Our new observations include a B supergiant in the Sextans B dwarf galaxy. The star SDSS J095951.18+052124.52 is located within the galaxy's 3′ Holmberg radius (Mateo 1998) and has a +295 ± 11 km s$^{-1}$ heliocentric radial velocity, consistent with the +295 ± 10 km s$^{-1}$ systemic velocity of Sextans B (Fisher & Tully 1975). The observed spectrum is that of a luminosity class I B supergiant. The $(m - M) = 25.6$ distance modulus of Sextans B (Piotto et al. 1994; Méndez et al. 2002) implies the star has $M_V = -6.25$, also consistent with a B I supergiant. We find no other B supergiants in our survey, suggesting that, to the depth

[1] IRAF is distributed by the National Optical Astronomy Observatory, which is operated by the Association of Universities for Research in Astronomy, Inc., under cooperative agreement with the National Science Foundation.

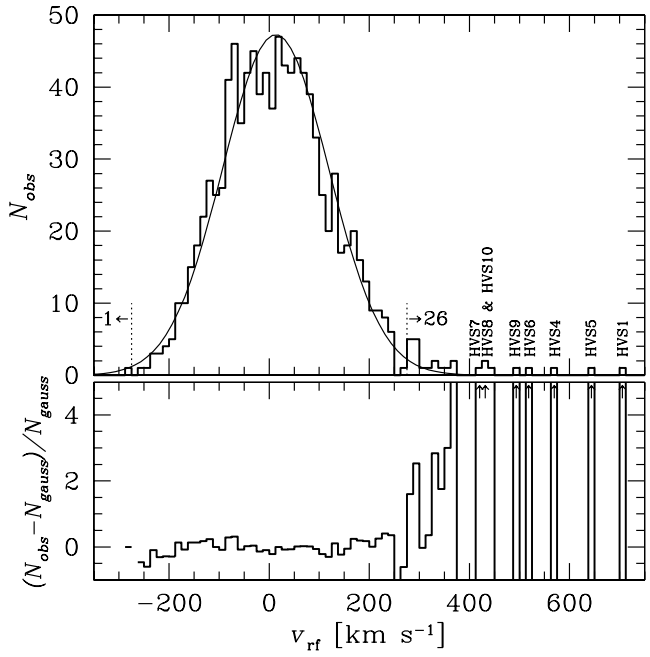


FIG. 2.—Galactic rest-frame velocity histogram for all 1005 B-type stars in our sample (*top*). The best-fit Gaussian (*thin line*) has dispersion 106 ± 4 km s$^{-1}$. The bottom panel plots the residuals of the observations from the best-fit Gaussian, normalized by the value of the Gaussian. The strong asymmetry of stars with $|v_{rf}| > 275$ km s$^{-1}$ is significant at the $\sim 5\,\sigma$ level, and shows that the bound stars with +300 km s$^{-1}$ are *short-lived*; we observe only one star falling back onto the Galaxy near −300 km s$^{-1}$.

of our survey, the census of star-forming dwarf galaxies in the Local Group may be complete over the region of sky covered by SDSS DR5.

In Figure 1 we also plot the Girardi et al. (2002, 2004) main-sequence track for a solar abundance 3 $M_\odot$ star (*lower solid line*) and a 4 $M_\odot$ star (*upper solid line*). If main-sequence stars fall in our survey, our color selection targets primarily 3–4 $M_\odot$ stars. All the HVSs overlap the main-sequence tracks within their 1 $\sigma$ uncertainties ($\sigma_{u'-g'} = \pm 0.042$, $\sigma_{g'-r'} = \pm 0.033$).

### 2.4. *Radial Velocity Distribution and Possibly Bound HVSs*

Figure 2 plots the distribution of line-of-sight velocities, corrected to the Galactic rest frame $v_{rf}$, for our entire sample of 1005 B-type stars. We calculate minimum Galactic rest-frame velocities by removing the radial component of the Sun's 220 km s$^{-1}$ orbital motion and the radial component of the Sun's motion with respect to the local standard of rest from the observed radial velocities (see Paper I).

The tail of positive velocity outliers in Figure 2 is truly striking: we observe 26 stars with $v_{rf} > 275$ km s$^{-1}$ and only 1 star with $v_{rf} < -275$ km s$^{-1}$. We estimate the significance of the asymmetric velocity distribution by fitting a Gaussian distribution to the data. We iteratively clip 3 $\sigma$ outliers and find a +13 ± 3 km s$^{-1}$ mean and a 106 ± 4 km s$^{-1}$ dispersion. The bottom panel of Figure 2 plots the residuals of the observations from this Gaussian distribution, normalized by the value of the Gaussian. Stars with velocities $|v_{rf}| < 275$ km s$^{-1}$ show low significance deviations from a Gaussian distribution and are likely a normal halo population (Paper I). Integrating the tail of the Gaussian suggests we should expect seven stars with $v_{rf} > 275$ km s$^{-1}$. Yet we observe 26 such objects, including the unbound HVSs. There is less than a $10^{-7}$ probability of drawing 26 stars with $v_{rf} > 275$ km s$^{-1}$ from a Gaussian distribution with the observed parameters. Thus the observed asymmetry appears significant at the 5 $\sigma$ level.

We now ask whether the nonzero mean of the distribution is consistent with models of HVS ejections. If the 19 objects in excess of the Gaussian distribution $v_{rf} > 275$ km s$^{-1}$ are HVSs, the Bromley et al. (2006) ejection model for 3 $M_\odot$ stars suggests that an additional 11 HVSs have $v_{rf} < 275$ km s$^{-1}$ in our survey. We randomly draw 30 objects from the Bromley et al. (2006) HVS ejection model and add them to 975 objects drawn from a Gaussian distribution with dispersion 106 km s$^{-1}$ and zero mean. The expected 30 HVSs shift the mean of the distribution by +2 ± 4 km s$^{-1}$, consistent with but not entirely sufficient to explain the observed shift in the mean.

In Paper II we argue that the significant excess of stars with velocities around $v_{rf} \sim +300$ km s$^{-1}$ demonstrates a population of HVSs ejected onto bound trajectories. HVS ejection mechanisms naturally produce a broad spectrum of ejection velocities that include bound orbits (Bromley et al. 2006). We observe 19 possibly bound HVSs with 275 km s$^{-1}$ $< v_{rf} <$ 400 km s$^{-1}$ in our completed survey. The colors of the bound HVSs suggest they are a mixed population: some of the bound HVSs are significantly redder or bluer than the main-sequence tracks (see Fig. 1). However, it is possible to pick a sample of ∼12 bound HVSs, the number in excess of the Gaussian distribution, that overlap the color distribution of the unbound HVSs. Follow-up spectroscopy is therefore required to constrain the stellar type of the possibly bound HVSs. Because we do not know which of the possibly bound HVSs are true HVSs, we focus our attention on the well-defined sample of unbound HVSs in this paper.

## 3. HYPERVELOCITY STARS

### 3.1. *Three New HVSs*

We discover three HVSs in our new observations. The objects are SDSS J094214.04+200322.07 (HVS8), SDSS J102137.08−005234.77 (HVS9), and SDSS J120337.86+180250.35 (HVS10). HVS8 has a B9 spectral type, a +512 ± 10 km s$^{-1}$ heliocentric radial velocity, and a minimum velocity of +430 km s$^{-1}$ in the Galactic rest frame. A solar metallicity 3 $M_\odot$ main-sequence star has $M_V \simeq -0.3$ (Schaller et al. 1992). This luminosity places HVS8 at a galactocentric distance $R = 53$ kpc. The mass of the Galaxy within 50 kpc is $5.5 \times 10^{11}$ $M_\odot$ (Wilkinson & Evans 1999; Sakamoto et al. 2003), which implies that the escape velocity at 50 kpc is ∼300 km s$^{-1}$. We conclude that HVS8 is very likely unbound to the Galaxy.

HVS9 has a B9 spectral type, a +632 ± 11 km s$^{-1}$ heliocentric radial velocity, and a minimum velocity of +489 km s$^{-1}$ in the Galactic rest frame. Unlike the other HVSs in our survey, which are located 10°–20° away on the sky from the nearest Local Group galaxy, HVS9 is 2.3° from the Sextans dwarf galaxy. Any physical association with Sextans is very unlikely, however. Sextans is 1320 ± 40 kpc distant (Dolphin et al. 2003) and has a heliocentric velocity of 224 ± 2 km s$^{-1}$ (Young 2000). Thus HVS9 is moving toward the dwarf galaxy with a relative velocity of 408 km s$^{-1}$. Interestingly, HVS9 also has the reddest $(g' - r')$ color of the HVSs; it is arguably the best blue horizontal branch (BHB) candidate among our HVSs. The equivalent width of its Ca II K line suggests low metallicity, and the Clewley et al. (2004) line-shape technique suggests low surface gravity. However, both measurements are notoriously uncertain at the hot effective temperature of HVS9, $(B - V) \simeq -0.01$. Whether HVS9 is a BHB star located at $R = 35$ kpc or a 3 $M_\odot$ main-sequence star at $R = 68$ kpc, its large velocity means it is certainly unbound.

HVS10 has a B9 spectral type, a +478 ± 10 km s$^{-1}$ heliocentric radial velocity, and a minimum velocity of +432 km s$^{-1}$ in the Galactic rest frame. HVS10 is the faintest HVS discovered

TABLE 1
HYPERVELOCITY STARS

| ID | Type | $M_V$ (mag) | $V$ (mag) | $R_{GC}$ (kpc) | $l$ (deg) | $b$ (deg) | $v_\odot$ (km s$^{-1}$) | $v_{rf}$ (km s$^{-1}$) | $t_{GC}$ (Myr) | Catalog | Reference |
|---|---|---|---|---|---|---|---|---|---|---|---|
| HVS1..... | B | −0.3 | 19.84 | 111 | 227.33 | +31.33 | 840 | 696 | 145 | SDSS J090744.99+024506.9 | 1 |
| HVS2..... | sdO | +2.6 | 19.05 | 26 | 175.99 | +47.05 | 708 | 717 | 32 | US 708 | 2 |
| HVS3..... | B | −2.7 | 16.20 | 62 | 263.04 | −40.91 | 723 | 548 | 100 | HE 0437−5439 | 3 |
| HVS4..... | B | −0.9 | 18.50 | 82 | 194.76 | +42.56 | 611 | 567 | 125 | SDSS J091301.01+305119.8 | 4 |
| HVS5..... | B | −0.3 | 17.70 | 45 | 146.23 | +38.70 | 551 | 647 | 60 | SDSS J091759.48+672238.3 | 4 |
| HVS6..... | B | −0.3 | 19.11 | 78 | 243.12 | +59.56 | 626 | 528 | 130 | SDSS J110557.45+093439.5 | 5 |
| HVS7..... | B | −0.9 | 17.80 | 56 | 263.83 | +57.95 | 534 | 421 | 110 | SDSS J113312.12+010824.9 | 5 |
| HVS8..... | B | −0.3 | 18.09 | 53 | 211.70 | +46.33 | 511 | 429 | 100 | SDSS J094214.04+200322.1 | ... |
| HVS9..... | B | −0.3 | 18.76 | 68 | 244.63 | +44.38 | 628 | 485 | 120 | SDSS J102137.08−005234.8 | ... |
| HVS10..... | B | −0.3 | 19.36 | 87 | 249.93 | +75.72 | 478 | 432 | 165 | SDSS J120337.85+180250.4 | ... |

REFERENCES.—(1) Brown et al. 2005; (2) Hirsch et al. 2005; (3) Edelmann et al. 2005; (4) Brown et al. 2006a; (5) Paper I.

by this survey, $g' = 19.295 \pm 0.024$, and is thus the most distant HVS known except for HVS1. Assuming it is a 3 $M_\odot$ main-sequence star, HVS10 is ∼84 kpc above the Galactic plane at its latitude $b = +76^\circ$.

Table 1 summarizes the HVS properties. Columns include HVS number, stellar type, inferred absolute magnitude $M_V$, apparent $V$ magnitude derived from SDSS photometry, galactocentric distance $R$, Galactic coordinates $(l, b)$, heliocentric radial velocity $v_\odot$, minimum Galactic rest-frame velocity $v_{rf}$ (not a full space velocity), travel time estimate from the Galactic center $t_{GC}$, and catalog identification. Velocities have changed slightly from previous work because we have obtained multiple observations of all the HVSs; here we report the weighted average of the velocity measurements. We include HVS1, HVS2, and HVS3 in Table 1 but exclude them from our analyses; the first three HVSs do not fall within the color/magnitude bounds of this targeted survey.

We do not report errors in Table 1 because formal uncertainties are misleadingly small compared to the (unknown) systematic errors. For example, heliocentric radial velocities are accurate to $\pm 11$ km s$^{-1}$, but we have no constraint on the proper-motion component of the rest-frame velocity $v_{rf}$. The luminosity estimates described below are precise to the 10% level for main-sequence stars; however, the luminosity estimates could be overestimated by an order of magnitude for post-main-sequence stars.

### 3.2. *Constraints on HVS Binaries*

Approximately 25% of late B-type stars in the solar neighborhood are in binaries with periods <100 days and with mass ratios greater than $m_2/m_1 > 0.1$ (Wolff 1978). Thus in principle, $2 \pm 1$ of the eight late B-type HVSs (we include HVS1) could be spectroscopic binaries. Although HVSs are ejected as single stars by standard HVS mechanisms, Lu et al. (2007) argue that the MBH binary mechanism can eject a compact HVS binary. Detection of a single HVS binary might thus provide compelling evidence for a binary MBH in the Galactic center (Lu et al. 2007).

We have two spectroscopic observations of each of the seven HVSs in this survey, typically obtained a few months apart. In all cases, the radial velocities are identical within the accuracy of the measurements, $\pm 11$ km s$^{-1}$. Thus it appears unlikely that the HVSs are compact binaries. We test this claim by comparing the observations with velocities drawn $10^4$ times from a typical 50 km s$^{-1}$ semiamplitude binary with random orbital phase and inclination. A Kolmogorov-Smirnov (K-S) test finds a 0.04 likelihood of drawing the observations from a binary system with 50 km s$^{-1}$ semiamplitude. Additional observations of higher accuracy are necessary to rule out radial velocity variations completely.

We have also obtained three observations of HVS1 spread over 3.5 yr. The heliocentric radial velocities are $853 \pm 12$, $816 \pm 14$, and $832 \pm 13$ km s$^{-1}$. Thus HVS1 may have velocity variations. However, HVS1 is a slowly pulsating B variable (Fuentes et al. 2006). Slowly pulsating B variables exhibit radial velocity amplitudes of ∼20 km s$^{-1}$ (Aerts et al. 1999; Mathias et al. 2001), consistent with the observations. Although our current observations are not conclusive, it is unlikely that any of the known HVSs are compact binary systems.

### 3.3. *HVS Template Spectrum*

Summing our HVS spectra allows construction of a high S/N template of the HVSs. Figure 3 displays the weighted average of our observations of HVS1 and HVS4–HVS10, shifted to the rest frame. The total integration time is equivalent to 4 hr on the 6.5 m MMT telescope. The strongest spectral features in Figure 3 are the hydrogen Balmer lines, visible from Hγ to H17.

It is interesting to discuss spectral classification in light of the weak spectral lines visible in Figure 3. The strengths of Mg II λ 4481 and the Si IIλ 4130 blend relative to He Iλ 4471 and He I λ 4144, respectively, indicate that the summed HVS spectrum must be later than a B7 spectral type. Notably, Ca IIλ 3933 and

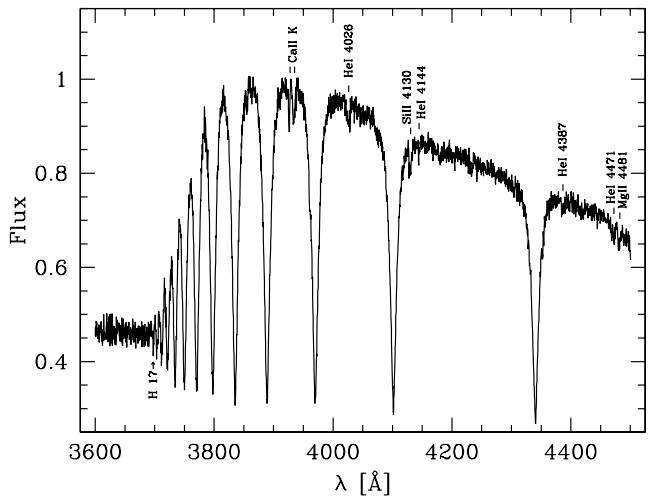


FIG. 3.—Summed HVS spectrum, created from the weighted average of our observations of HVS1 and HVS4–HVS10, shifted to rest frame. The spectral type is that of a B8–B9 star. The wavelength difference between the pair of Ca II K lines, one from the HVSs and one from the local interstellar medium that appears in the spectra of HVS8 and HVS9, visibly indicates the large space motion of the HVSs, $\Delta\lambda/\lambda \sim 550$ km s$^{-1}$.

He I$\lambda$ 4026 have similar equivalent widths, indicating that the summed HVS spectrum has a spectral type of B8–B9. This late B spectral type is consistent with our color selection and our previous spectral classifications.

Amusingly, we also see two Ca II K lines in Figure 3. One Ca II K line is from the atmospheres of the HVSs at 3933 Å, and the other is from the local interstellar medium in the direction of HVS8 and HVS9. The interstellar Ca II K line appears shifted to 3926 Å in the rest frame of HVS8 and HVS9. The difference between the two Ca II K lines, $\Delta\lambda/\lambda \sim 550$ km s$^{-1}$, visibly indicates the large space motion of the HVSs.

## 4. NATURE OF THE HYPERVELOCITY STARS

We use the observed velocity distribution (Fig. 2) to show that HVSs must be short-lived. Using stellar evolution arguments and orbit calculations, we argue that the HVSs are likely main-sequence stars.

### 4.1. *The Asymmetric Velocity Distribution*

The HVSs are moving away from us with large positive radial velocities 400 km s$^{-1}$ $< v_{\rm rf} <$ 700 km s$^{-1}$. As stated earlier, the escape velocity of the Galaxy at 50 kpc is $\sim$300 km s$^{-1}$, or 360 km s$^{-1}$ in the Bromley et al. (2006) model (see Fig. 4). Therefore, the absence of objects with $v_{\rm rf} < -400$ km s$^{-1}$ is no surprise: unbound HVSs will never come back.

The significant excess of +300 km s$^{-1}$ stars compared to $-300$ km s$^{-1}$ stars shows that the possibly bound HVSs *must be short-lived stars*: every star traveling at +300 km s$^{-1}$ must eventually fall back onto the Galaxy at roughly $-300$ km s$^{-1}$. Kollmeier & Gould (2007) and Yu & Madau (2007) also make this point. The return time depends on the apocenter of the orbits, and ranges from 800 to 2400 Myr for the range of distances and velocities we observe. Although a HVS's radial orbit may be altered by the asphericity of the Galactic potential (Yu & Madau 2007), the effect on radial velocity should be minor at the distances probed by our survey.

### 4.2. *HVSs are Main-Sequence Stars*

The stars we observe have the spectral types of B stars, but they may be main-sequence or post-main-sequence stars. After a main-sequence star exhausts its hydrogen fuel, it evolves up the red giant branch, ignites helium, and becomes a blue horizontal branch (BHB) star. All stars with masses capable of igniting helium burning, including turnoff stars in the halo, spend of order $10^8$ yr as BHB stars (Yi et al. 1997). The ambiguity in identifying BHB stars arises because the horizontal branch overlaps the main sequence at the effective temperatures of our late B-type stars, $T_{\rm eff} \sim 10^4$ K. Thus we cannot discriminate BHB and main-sequence stars by surface gravity alone.

In Paper I we use kinematics and metallicities to show that most of the B-type stars are consistent with a halo population of post-main-sequence stars or blue stragglers in the halo. The HVSs are a different class of objects. Thus the question stands: are the HVSs 3–4 $M_\odot$ main-sequence stars or BHB stars?

The colors we observe preferentially sample hot BHB stars with small hydrogen envelopes. Hot BHB stars are present in only 25% of globular clusters (Lee et al. 2007). One may wonder whether hot BHB stars are common in a Galactic center population with solar abundance (Carr et al. 2000; Ramírez et al. 2000; Cunha et al. 2007). Theoretical evolutionary tracks allow for BHB stars at all metallicities (Yi et al. 1997). Hot BHB stars may, in fact, be more common at high metallicities because increased opacity may cause increased mass loss in the red giant branch phase (Faulkner 1972). Evidence for this picture comes from the metal-rich [Fe/H] $\simeq +0.4$ open cluster NGC 6791, where a third of its helium-burning stars are hot BHB stars (Yong et al. 2000).

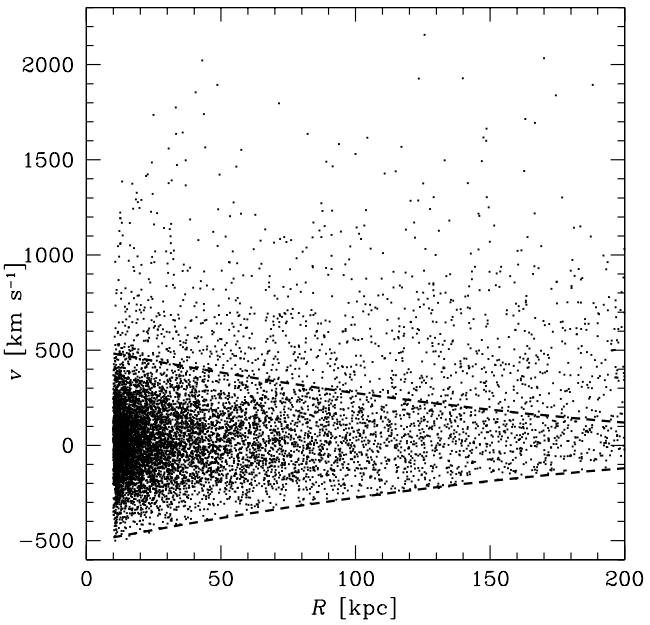


FIG. 4.—Distribution of distance and velocity of simulated 1 $M_\odot$ HVSs from the Bromley et al. (2006) ejection model. The dashed line indicates the approximate escape velocity of the potential. In the range 10 kpc $< R <$ 50 kpc, 95% of the simulated 1 $M_\odot$ HVSs are bound, and 2/3 have crossed the Galactic center multiple times. If HVSs are BHB stars, we should thus find approximately equal numbers of stars at +300 and $-300$ km s$^{-1}$, contrary to the observations.

It is unlikely, however, that a HVS is ejected during the horizontal branch phase. In the red giant phase, prior to becoming a BHB star, a star swells to a radius of $\sim$1 AU. HVS ejections from a single MBH require stellar binaries with separations of 0.1–1 AU (Hills 1988; Bromley et al. 2006). Thus any progenitor HVS system experiences a common-envelope phase that inspirals the binary system over $\lesssim 10^3$ yr (Webbink 2007) that probably prevents a HVS ejection by the time the star reaches the BHB phase. If HVSs are BHB stars, they must be ejected as main-sequence stars. This condition is relaxed for single stars ejected by a pair of MBHs or an inspiraling IMBH.

However, the lifetime constraint derived from the observed velocities means that the HVSs cannot be BHB stars descended from stars of mass less than 2 $M_\odot$. The progenitors of BHB stars span a wide range of stellar masses and include stars with main-sequence lifetimes up to a Hubble time. Thus low-mass HVSs ejected many gigayears ago may be observed as BHB stars in our survey. In Figure 4 we illustrate the spatial and velocity distribution of such a population from a simulation of 1 $M_\odot$ HVS ejections. Bromley et al. (2006) describe the details of the ejection model. In brief, we disrupt equal-mass binaries using the Hill's mechanism, and assume that the 1 $M_\odot$ stars are ejected at a random time during their main-sequence lifetime. For reference, we also show the approximate escape velocity of the potential model with dashed lines (Fig. 4).

Our magnitude-limited survey detects BHB stars in the range 10 kpc $< R <$ 50 kpc. Over this range of $R$, 95% of the simulated 1 $M_\odot$ HVSs are bound; 2/3 of them have crossed the Galactic center multiple times. Thus if HVSs are BHB stars, we should observe approximately equal numbers of BHB stars at +300 and $-300$ km s$^{-1}$, contrary to the observations (Fig. 2). We simply

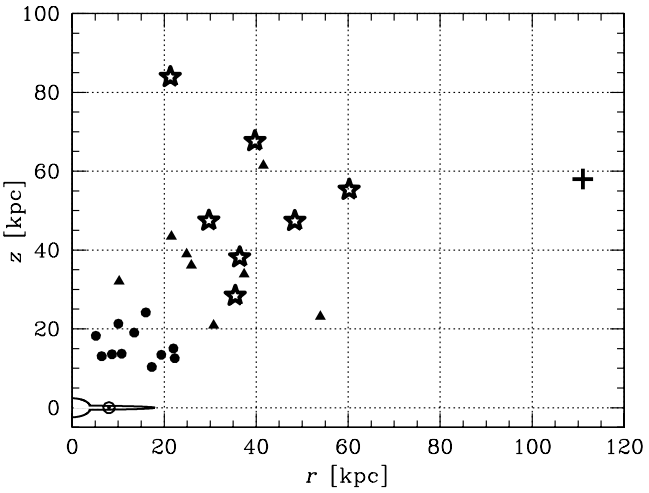


FIG. 5.—Location of our seven HVSs (*stars*), the possibly bound HVSs (*circles, triangles*), and HVS1 (*plus sign*) assuming they are main-sequence B stars; $z$ is the distance above the Galactic plane, and $r$ is the distance along the Galactic plane, such that $R = (r^2 + z^2)^{-0.5}$. For reference, we sketch the Milky Way and the Sun at $(r, z) = (8, 0)$ kpc.

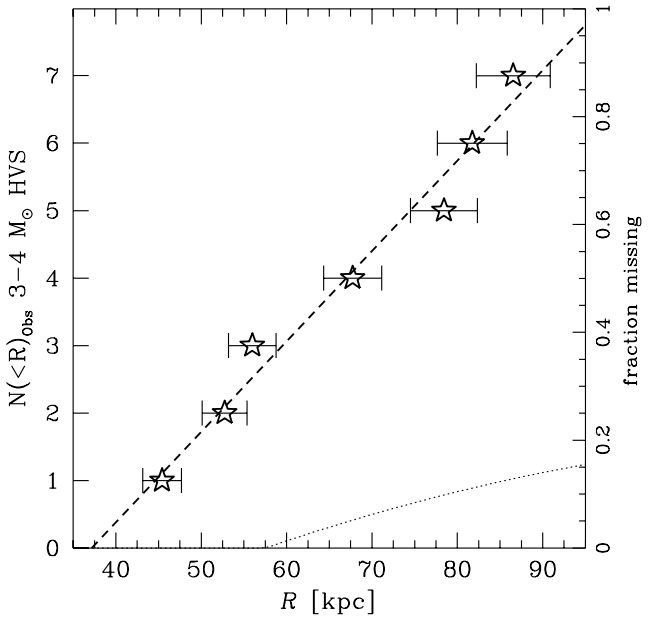


FIG. 6.—Observed distribution of HVSs (*stars*) vs. galactocentric radius $R$. Error bars indicate 10% luminosity uncertainties. The dotted line shows the fraction of HVSs with travel times exceeding their lifetime at distance $R$, indicated on the right-hand vertical axis. The best-fit line through the data (*dashed line*), corrected for incompleteness, has slope $0.159 \pm 0.017$ kpc$^{-1}$.

do not see BHB stars from long-lived progenitors falling back onto the Galaxy with large negative radial velocities.

Thus HVSs must have main-sequence lifetimes less than the $\sim$1 Gyr turnaround time. Given the color selection of our survey, the HVSs are either 3–4 $M_\odot$ main-sequence stars, or possibly hot BHB stars evolved from $M > 2\ M_\odot$ progenitors. Our understanding of $M > 2\ M_\odot$ BHB stars is limited by the absence of stellar evolution tracks that connect the zero-age main sequence mass to the horizontal branch core mass. Main-sequence stars, on the other hand, match the current understanding of the Galactic center: Maness et al. (2007) find evidence for a top-heavy initial mass function in the Galactic center, and Eisenhauer et al. (2005) show that the stars presently in orbit around the central MBH are main-sequence B stars, some of which may be the former companions of the HVSs (Ginsburg & Loeb 2006, 2007). The 3–4 $M_\odot$ main-sequence stars sampled by our survey have lifetimes of 160–350 Myr, consistent with the absence of bound HVSs falling back onto the Galaxy with large negative velocities. We conclude that HVSs are likely main-sequence stars.

## 5. SPACE DENSITY OF HYPERVELOCITY STARS

Our essentially complete survey places interesting constraints on the space density of HVSs. The presence of a MBH in the Galactic center inevitably ejects a fountain of HVSs from the Galaxy. If HVS ejections are continuous and isotropic, their space density should be proportional to $R^{-2}$ (see also B. C. Bromley et al. 2008, in preparation). The volume sampled by our survey is proportional to $R^3$. Thus in the simplest picture, we expect the number of HVSs in our survey to have the dependence $N(<R) \propto R$. The actual space density depends on the luminosities of the HVSs. We use the space density to predict HVS discoveries for future surveys.

### 5.1. *HVS Luminosities and Distances*

Having established that HVSs are likely main-sequence stars, we estimate their intrinsic luminosities from Schaller et al. (1992) stellar evolutionary tracks for solar metallicity stars. Five of the HVSs in our survey have colors (see Fig. 1) and spectra consistent with 3 $M_\odot$ stars; the two bluest HVSs are consistent with 4 $M_\odot$ stars. Using bolometric corrections from Kenyon & Hartmann (1995) we estimate $M_V(3\ M_\odot) \simeq -0.3$ and $M_V(4\ M_\odot) \simeq -0.9$. These absolute magnitudes put the HVSs at distances in the range 45 kpc $< R <$ 90 kpc.

Figure 5 illustrates the HVS's location in the outer halo of the Galaxy. The possibly bound HVSs, in contrast, are mostly found at closer distances; there are 11 possibly bound HVSs and no unbound HVS in the bright FAST sample. Given a $N(<R) \propto R$ distribution, one may wonder why there are no unbound HVSs nearby. Projection effects may provide one explanation. Consider SDSS J144955.58+310351.4 (highlighted in Paper II), a possibly bound HVS located at $R \simeq 17$ kpc and traveling $v_{\rm rf} = +447$ km s$^{-1}$. If SDSS J144955.58+310351.4 has a purely radial trajectory, its true space velocity is +525 km s$^{-1}$, and it may thus be unbound. But because we do not know which of the possibly bound HVSs are true HVSs, we use only the well-defined sample of unbound HVSs below.

We next compare the HVS distances with the range of distances sampled by our magnitude-limited survey. Our survey is complete over the magnitude range $15 < g_0' < 19.5$, corresponding to heliocentric distances of 12 kpc $< d <$ 100 kpc and 16 kpc $< d <$ 130 kpc for 3 and 4 $M_\odot$ stars, respectively. The range of galactocentric $R$ varies with Galactic latitude and longitude on the sky. Over our 7300 deg$^2$ survey region, we are complete over the range 20 kpc $< R <$ 93 kpc and 24 kpc $< R <$ 124 kpc for 3 and 4 $M_\odot$ stars, respectively. The inner edge of the MMT survey, in which the HVSs are found, is located at $R = 38$ and $R = 48$ kpc for 3 and 4 $M_\odot$ stars, respectively.

Figure 6 plots the cumulative distribution of distances for the seven HVSs in this survey. The distribution is remarkably consistent with a continuous ejection process: a K-S test finds a 0.96 likelihood of drawing the distribution of HVSs from a linear distribution $N(<R) \propto R$. This conclusion is independent of the absolute scale of $R$.

### 5.2. *Lifetime Correction*

Before computing the space density of HVSs from Figure 6, we must correct for the number of HVSs missing in our survey because of their finite lifetimes. Using the ejection models of

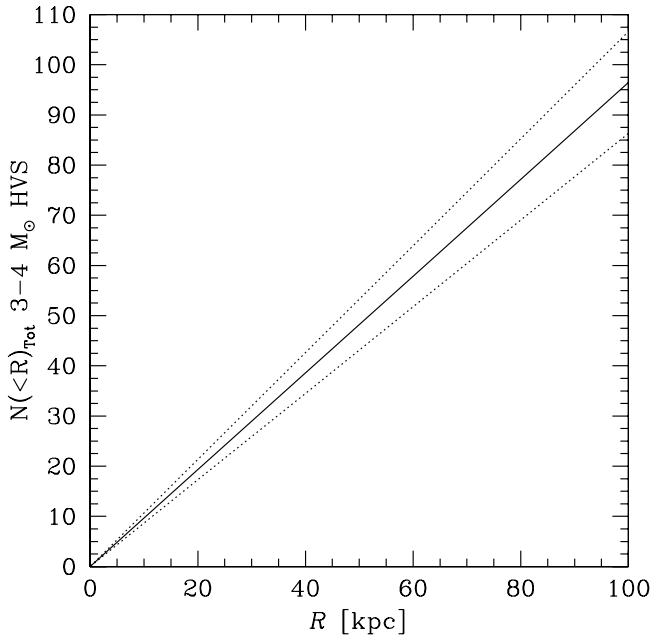


FIG. 7.—Cumulative number of 3–4 $M_\odot$ HVSs vs. galactocentric radius $R$. Over $4\pi$ sr, the space density of 3–4 $M_\odot$ HVSs is $\rho(R) = (0.077 \pm 0.008)R^{-2}$ kpc$^{-3}$. We infer there are $96 \pm 10$ 3–4 $M_\odot$ HVSs within $R < 100$ kpc.

Bromley et al. (2006) we calculate the fraction of stars with $v > v_{\rm esc}$ at a given $R$ with travel times exceeding their lifetimes. The dotted line in Figure 6 shows the weighted average of the 3 and 4 $M_\odot$ correction factors, appropriate for our set of HVSs.

The lifetime correction is negligible for 3 $M_\odot$ HVSs in our magnitude range, but it is substantial for the faintest 4 $M_\odot$ HVSs. The two 4 $M_\odot$ HVSs in our survey are located at $R = 56$ and $R = 82$ kpc; given a $N(< R) \propto R$ dependence, we expect to find one or two more 4 $M_\odot$ HVSs out to $R = 124$ kpc. However, the Bromley et al. (2006) ejection models show that 50% of unbound 4 $M_\odot$ HVSs are dead by $R = 90$ kpc, and 67% are dead by $R = 110$ kpc. Thus the absence of 4 $M_\odot$ HVSs with $R > 90$ kpc is consistent with the interpretation that they are main-sequence stars with short, 160 Myr lifetimes. The 3 $M_\odot$ HVSs, on the other hand, fill the region where we can detect them, consistent with their longer, 350 Myr main-sequence lifetimes.

### 5.3. *Density Distribution*

We derive the HVS space density from a least-squares fit to the observations, corrected for lifetime. The slope is $0.159 \pm 0.017$ kpc$^{-1}$ (see Fig. 6). We estimate the uncertainty by assigning random uncertainties to the HVSs, drawn from a Gaussian distribution with $\sigma = 10\%$ in luminosity, and by refitting the line $10^4$ times. Because all seven HVSs have $g_0' > 17$, they are drawn from the MMT survey and cover an effective area of 6800 deg$^2$ of sky (93% of 7300 deg$^2$). Corrected to $4\pi$ sr, the space density of 3–4 $M_\odot$ HVSs is thus $\rho(R) = (0.077 \pm 0.008)R^{-2}$ kpc$^{-3}$.

Figure 7 plots the cumulative number of 3–4 $M_\odot$ HVSs in the Galaxy. Our observations imply there are $96 \pm 10$ late B-type HVSs in the sphere $R < 100$ kpc, about 1 HVS kpc$^{-1}$.

### 5.4. *Prediction for Future Surveys*

We can use the space density of 3–4 $M_\odot$ HVSs to predict HVS detections in future surveys. Our predictions make the following assumptions. (1) We assume that the distribution of HVS velocities is the same for all stellar masses. Ejection velocity depends weakly on the mass of the stellar binary $(m_1 + m_2)^{1/3}$ in the Hill's mechanism, but there is no such dependence for stars ejected from a binary MBH. (2) We use the Salpeter mass function, $M^{-2.35}$ (Salpeter 1955), and the present-day mass function of the bulge, $M^{-4.5}$ for $M > 1$ $M_\odot$ and $M^{-2.35}$ for $M < 1$ $M_\odot$ (Mezger et al. 1999), as two representative mass functions for calculating the number ratios of stars of different stellar masses. (3) If HVSs are ejected by the Hill's mechanism, we implicitly assume that the same fraction of stars are in compact binaries at all masses; no such assumption is required for the binary MBH mechanism. (4) We use the Girardi et al. (2004) stellar isochrones of solar abundance to obtain luminosities for stars at a given mass, or color. We use the luminosities to calculate survey volumes for a set of magnitude limits. (5) Finally, we assume observation of 100% of stars in a given area of sky.

Kollmeier & Gould (2007) propose observing faint $19.5 < g' < 21.5$ stars near the main-sequence turnoff $0.3 < (g' - i') < 1.1$ as the optimal strategy for finding low-mass HVSs. The $(g' - i')$ colors select 0.8 $M_\odot < M < 1.3$ $M_\odot$ solar metallicity stars with absolute magnitudes $3.7 < M_V < 6.3$. Using the present-day mass function of the bulge, we estimate that there is one HVS $\sim$50 deg$^{-2}$ in the proposed magnitude range, in excellent agreement with the one HVS 45 deg$^{-2}$ estimated by Kollmeier & Gould (2007). However, a Salpeter mass function predicts an order-of-magnitude lower density, one HVS $\sim$500 deg$^{-2}$. The ratio of high- to low-mass HVSs thus provides a sensitive measure of the stellar mass function near the central MBH (Kollmeier & Gould 2007; B. C. Bromley et al. 2008, in preparation).

The Sloan Extension for Galactic Understanding and Exploration (SEGUE) is an ongoing survey that includes spectroscopy of 1144 stars along $\sim$200 sight lines with the SDSS telescope (Adelman-McCarthy et al. 2008). Each sight line covers 7 deg$^2$ of sky, for a total of 1400 deg$^2$ of spectroscopic coverage. Notably, SEGUE acquires spectra for 150 BHB/A-type stars per sight line over the magnitude range $14 < g' < 20.5$. The BHB/A color cut (Adelman-McCarthy et al. 2008) selects for 1.5 $M_\odot < M <$ 2.5 $M_\odot$ stars with absolute magnitudes $0.7 < M_V < 2.8$. We estimate SEGUE should find $\sim$5 to $\sim$15 HVSs for the Salpeter and present-day mass functions, respectively. However, if only a fraction of BHB/A stars are observed over the 1400 deg$^2$ area, or if the spectra are not reliable to a depth $g' = 20.5$, our predictions may be overestimates.

SEGUE also targets F/G-type stars over the magnitude range $14 < g' < 20.2$. If we ignore low-metallicity targets as unlikely HVS candidates, SEGUE targets 50 F/G main-sequence stars per sight line. The color cut $0.2 < (g' - r') < 0.48$ (Adelman-McCarthy et al. 2008) selects for 1.1 $M_\odot < M <$ 1.4 $M_\odot$ stars with absolute magnitudes $3.0 < M_V < 4.6$. We estimate that 50 stars per sight line account for $\sim$10% of the total population of F/G stars, based on number counts of stars in stripe 82. We estimate that SEGUE should find $\sim$0.1 to $\sim$1 F/G-type HVS for the Salpeter and present-day mass functions, respectively. The F/G-type HVS discovery rate is low because SEGUE is not complete for F/G stars and because F/G stars have intrinsically low luminosity.

Regardless of stellar type, future HVS discoveries require surveys that (1) sample large areas of sky $\gg 10^2$ deg$^2$ and (2) sample large depths $R \gg 10$ kpc. As a practical matter, the HVSs must also have a high contrast with respect to the indigenous stellar population for efficient detection. Our HVS survey is successful because late B-type stars are luminous, and because the contamination from evolved BHB stars and their low-mass progenitors is minimal, $\sim$100 halo stars per HVS.

## 6. EJECTION HISTORY OF HYPERVELOCITY STARS

Knowing the distances and velocities of the HVSs, we can estimate their travel times from the Galactic center. Although we

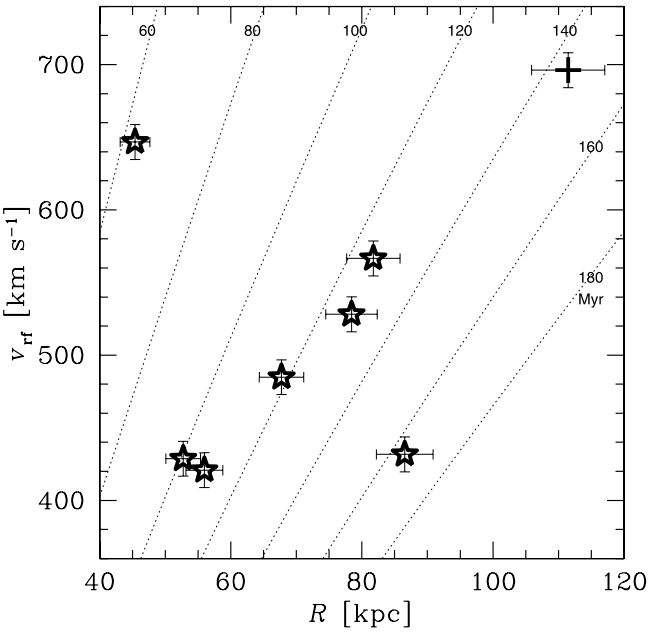


FIG. 8.— Minimum rest-frame velocity and distance of the HVSs (*stars*) and HVS1 (*plus sign*). Error bars indicate the precision of the measurements; systematic errors may be larger. Travel times from the Galactic center (*dotted lines*) are calculated using the potential model of Bromley et al. (2006) and assuming the minimum rest-frame velocity $v_{rf}$ is the full space motion of the stars. The distribution of travel times statistically favor a constant ejection rate, although a 120 Myr old burst of HVSs is also allowed.

do not know the HVSs' true space motions, at large distances their motion should be mostly radial. Thus we calculate travel times assuming the HVSs' minimum rest-frame velocities are their full space motions. This assumption means the travel time estimates are in fact upper limits. We use the potential model of Bromley et al. (2006) to correct for the deceleration of the HVSs. The deceleration correction reduces travel times by 10% compared to travel times calculated assuming constant velocity (as reported in Paper I). Table 1 lists travel time estimates for HVS4–HVS10 and HVS1, although we do not include HVS1 in this analysis. Figure 8 plots the distribution of travel times.

The HVSs sample the ejection history of stars from the Galactic center over the past $\sim$165 Myr. The HVS travel times might favor a single burst, like that expected from the inspiral of a binary MBH, or a continuous ejection process, as expected from Hill's mechanism. Interestingly, five of the seven HVS travel times appear clustered around 120 Myr. A K-S test finds a 0.8 likelihood of drawing all seven HVSs from a linear distribution in time, and a 0.2 likelihood of drawing them from a single burst (e.g., travel times that fall along the dotted line marked 120 Myr in Fig. 8).

The statistics appear to favor a continuous ejection process. Thus Hill's mechanism can plausibly account for the entire set of observed HVSs. A single burst event is also allowed, however. If HVSs were ejected from the inspiral of a binary MBH, the observations suggest such an event may have occurred $\sim$120 Myr ago. We caution that small-number statistics prevent any strong conclusion; additional HVS discoveries are required to properly constrain the ejection history of stars from the Galactic center.

## 7. CONCLUSIONS

Our targeted HVS survey, a spectroscopic survey of stars with B-type colors, is 96.5% complete over 7300 deg$^2$ of the SDSS DR5. We report three new HVS discoveries, for a total of seven HVSs with $15 < g_0' < 19.5$ over a sixth of the sky. In addition, we find 19 possibly bound HVSs with velocities 275 km s$^{-1}$ $< v_{rf} < 400$ km s$^{-1}$.

The significant excess of +300 km s$^{-1}$ stars compared to $-300$ km s$^{-1}$ stars shows that the HVSs must be short-lived. Any population of post-main-sequence HVSs must contain stars falling back onto the Galaxy, contrary to the observations. We conclude the HVSs are likely 3–4 $M_\odot$ main-sequence stars, although hot BHB stars from $M > 2$ $M_\odot$ progenitors are also a possibility. Observations of stars in the central 10 pc of the Galaxy are now probing $\sim$3 $M_\odot$ main-sequence stars, some of which may feed the MBH and produce HVSs. Thus there is a need to better understand the BHB phase of 2–3 $M_\odot$ stars in the context of HVSs and Galactic center research.

The spatial distribution of HVSs supports the main-sequence interpretation. The longer lived 3 $M_\odot$ HVSs fill our survey volume; the shorter lived 4 $M_\odot$ HVSs are missing at faint magnitudes. The spatial distribution of HVSs is remarkably consistent with a $N(< R) \propto R$ distribution, as expected for a continuous ejection process. The density of 3–4 $M_\odot$ HVSs is $\rho(R) = (0.077 \pm 0.008)R^{-2}$ kpc$^{-3}$, implying a total of $96 \pm 10$ such HVSs within $R < 100$ kpc.

A sample of $\gtrsim$100 HVSs is required to discriminate among HVS ejection mechanisms and Galactic potential models (Sesana et al. 2007a). Thus enough 3–4 $M_\odot$ HVSs may exist in the Galaxy to test the ejection and potential models, especially if the bound HVSs can be used. SEGUE and other future surveys will find more HVSs and will allow further use of this important class of objects to connect the Galactic center to the Galactic halo.

We thank M. Alegria, J. McAfee, and A. Milone for their assistance with observations obtained at the MMT Observatory, a joint facility of the Smithsonian Institution and the University of Arizona. We thank the referee for comments that improved this paper. This project makes use of data products from the Sloan Digital Sky Survey, which is managed by the Astrophysical Research Consortium for the Participating Institutions. This research has made use of NASA's Astrophysics Data System Bibliographic Services. This work was supported by the Smithsonian Institution.

*Facilities:* FLWO:1.5m (FAST Spectrograph), MMT (Blue Channel Spectrograph)

## APPENDIX

## DATA TABLE

Table 2 lists the 381 new observations from our HVS survey, excluding the extragalactic objects; 206 HVS candidates were observed with the MMT, and 175 were observed with FAST (see § 2). Table 2 includes columns of right ascension (R.A.) and declination (Decl.) coordinates (J2000.0), $g'$ apparent magnitude, $(u' - g')_0$ and $(g' - r')_0$ color, and our heliocentric velocity $v_\odot$. The column WD indicates whether the object is a white dwarf (WD = 1) or a B-type star (WD = 0).

TABLE 2
HVS Survey: New Observations

| R.A. (J2000.0) | Decl. (J2000.0) | $g'$ (mag) | $(u'-g')_0$ (mag) | $(g'-r')_0$ (mag) | WD | $v_\odot$ (km s$^{-1}$) |
|---|---|---|---|---|---|---|
| 0 23 09.05..... | −0 33 42.0 | 16.277 ± 0.020 | 0.250 ± 0.028 | −0.306 ± 0.039 | 1 | −13 ± 31 |
| 0 23 53.29..... | −1 04 46.4 | 18.304 ± 0.016 | 0.749 ± 0.042 | −0.255 ± 0.025 | 0 | 20 ± 10 |
| 0 43 50.55..... | −9 52 27.0 | 16.326 ± 0.032 | 0.832 ± 0.038 | −0.358 ± 0.038 | 0 | −117 ± 11 |

Note.—Units of right ascension are hours, minutes, and seconds, and units of declination are degrees, arcminutes, and arcseconds. Table 2 is published in its entirety in the electronic edition of the *Astrophysical Journal*. A portion is shown here for guidance regarding its form and content.

REFERENCES


Adelman-McCarthy, J. K., et al. 2007, ApJS, 172, 634
———. 2008, ApJS, 175, in press (arXiv: 0707.3413v2)
Aerts, C., et al. 1999, A&A, 343, 872
Baumgardt, H., Gualandris, A., & Portegies Zwart, S. 2006, MNRAS, 372, 174
Blaauw, A. 1961, Bull. Astron. Inst. Netherlands, 15, 265
Bromley, B. C., Kenyon, S. J., Geller, M. J., Barcikowski, E., Brown, W. R., & Kurtz, M. J. 2006, ApJ, 653, 1194
Brown, W. R., Allende Prieto, C., Beers, T. C., Wilhelm, R., Geller, M. J., Kenyon, S. J., & Kurtz, M. J. 2003, AJ, 126, 1362
Brown, W. R., Geller, M. J., Kenyon, S. J., & Kurtz, M. J. 2005, ApJ, 622, L33
———. 2006a, ApJ, 640, L35
———. 2006b, ApJ, 647, 303 (Paper I)
———. 2007a, ApJ, 666, 231
Brown, W. R., Geller, M. J., Kenyon, S. J., Kurtz, M. J., & Bromley, B. C. 2007b, ApJ, 660, 311 (Paper II)
Brown, W. R., Kewley, L. J., & Geller, M. J. 2008, AJ, in press (arXiv: 0709.4400v1)
Carr, J. S., Sellgren, K., & Balachandran, S. C. 2000, ApJ, 530, 307
Clewley, L., Warren, S. J., Hewett, P. C., Norris, J. E., & Evans, N. W. 2004, MNRAS, 352, 285
Cunha, K., Sellgren, K., Smith, V. V., Ramirez, S. V., Blum, R. D., & Terndrup, D. M. 2007, ApJ, 669, 1011
Davies, M. B., King, A., & Ritter, H. 2002, MNRAS, 333, 463
Demarque, P., & Virani, S. 2007, A&A, 461, 651
Dolphin, A. E., et al. 2003, AJ, 125, 1261
Edelmann, H., Napiwotzki, R., Heber, U., Christlieb, N., & Reimers, D. 2005, ApJ, 634, L181
Eisenhauer, F., et al. 2005, ApJ, 628, 246
Fabricant, D., Cheimets, P., Caldwell, N., & Geary, J. 1998, PASP, 110, 79
Faulkner, J. 1972, ApJ, 173, 401
Fisher, J. R., & Tully, R. B. 1975, A&A, 44, 151
Fuentes, C. I., Stanek, K. Z., Gaudi, B. S., McLeod, B. A., Bogdanov, S., Hartman, J. D., Hickox, R. C., & Holman, M. J. 2006, ApJ, 636, L37
Ghez, A. M., Salim, S., Hornstein, S. D., Tanner, A., Lu, J. R., Morris, M., Becklin, E. E., & Duchene, G. 2005, ApJ, 620, 744
Ginsburg, I., & Loeb, A. 2006, MNRAS, 368, 221
———. 2007, MNRAS, 376, 492
Girardi, L., Bertelli, G., Bressan, A., Chiosi, C., Groenewegen, M. A. T., Marigo, P., Salasnich, B., & Weiss, A. 2002, A&A, 391, 195
Girardi, L., Grebel, E. K., Odenkirchen, M., & Chiosi, C. 2004, A&A, 422, 205
Gnedin, O. Y., Gould, A., Miralda-Escudé, J., & Zentner, A. R. 2005, ApJ, 634, 344
Gualandris, A., & Portegies Zwart, S. 2007, MNRAS, 376, L29
Gualandris, A., Portegies Zwart, S. P., & Sipior, M. S. 2005, MNRAS, 363, 223
Hills, J. G. 1988, Nature, 331, 687
Hirsch, H. A., Heber, U., O'Toole, S. J., & Bresolin, F. 2005, A&A, 444, L61
Kenyon, S. J., & Hartmann, L. 1995, ApJS, 101, 117
Kewley, L. J., Brown, W. R., Geller, M. J., Kenyon, S. J., & Kurtz, M. J. 2007, AJ, 133, 882
Kilic, M., Allende Prieto, C., Brown, W. R., & Koester, D. 2007a, ApJ, 660, 1451
Kilic, M., Brown, W. R., Allende Prieto, C., Pinsonneault, M., & Kenyon, S. 2007b, ApJ, 664, 1088
Kollmeier, J. A., & Gould, A. 2007, ApJ, 664, 343
Kurtz, M. J., & Mink, D. J. 1998, PASP, 110, 934
Lee, Y.-W., Gim, H. B., & Casetti-Dinescu, D. I. 2007, ApJ, 661, L49
Leonard, P. J. T. 1991, AJ, 101, 562
———. 1993, in ASP Conf. Ser. 45, Luminous High-Latitude Stars, ed. D. Sasselov (San Francisco: ASP), 360
Levin, Y. 2006, ApJ, 653, 1203
Lu, Y., Yu, Q., & Lin, D. N. C. 2007, ApJ, 666, L89
Maness, H., et al. 2007, ApJ, 669, 1024
Mateo, M. L. 1998, ARA&A, 36, 435
Mathias, P., Aerts, C., Briquet, M., De Cat, P., Cuypers, J., Van Winckel, H., & Le Contel, J. M. 2001, A&A, 379, 905
Méndez, B., Davis, M., Moustakas, J., Newman, J., Madore, B. F., & Freedman, W. L. 2002, AJ, 124, 213
Merritt, D. 2006, ApJ, 648, 976
Mezger, P. G., Zylka, R., Philipp, S., & Launhardt, R. 1999, A&A, 348, 457
O'Leary, R. M., & Loeb, A. 2008, MNRAS, in press (astro-ph/0609046)
Perets, H. B., & Alexander, T. 2007, ApJ, submitted (arXiv: 0705.2123v1)
Perets, H. B., Hopman, C., & Alexander, T. 2007, ApJ, 656, 709
Piotto, G., Capaccioli, M., & Pellegrini, C. 1994, A&A, 287, 371
Portegies Zwart, S. F. 2000, ApJ, 544, 437
Poveda, A., Ruiz, J., & Allen, C. 1967, Bol. Obs. Tonantzintla Tacubaya, 4, 86
Ramírez, S. V., Sellgren, K., Carr, J. S., Balachandran, S. C., Blum, R., Terndrup, D. M., & Steed, A. 2000, ApJ, 537, 205
Sakamoto, T., Chiba, M., & Beers, T. C. 2003, A&A, 397, 899
Salpeter, E. E. 1955, ApJ, 121, 161
Schaller, G., Schaerer, D., Meynet, G., & Maeder, A. 1992, A&AS, 96, 269
Schödel, R., Ott, T., Genzel, R., Eckart, A., Mouawad, N., & Alexander, T. 2003, ApJ, 596, 1015
Sesana, A., Haardt, F., & Madau, P. 2006, ApJ, 651, 392
———. 2007a, ApJ, 660, 546
———. 2007b, MNRAS, 379, L45
Tauris, T. M., & Takens, R. J. 1998, A&A, 330, 1047
Webbink, R. F. 2007, in Short Period Binary Stars, ed. E. F. Milone, D. A. Leahy, & D. W. Hobill (Berlin: Springer), submitted (arXiv: 0704.0280v1)
Wilkinson, M. I., & Evans, N. W. 1999, MNRAS, 310, 645
Wolff, S. C. 1978, ApJ, 222, 556
Yi, S., Demarque, P., & Kim, Y.-C. 1997, ApJ, 482, 677
Yong, H., Demarque, P., & Yi, S. 2000, ApJ, 539, 928
Young, L. M. 2000, AJ, 119, 188
Yu, Q., & Madau, P. 2007, MNRAS, 379, 1293
Yu, Q., & Tremaine, S. 2003, ApJ, 599, 1129